An implicit method for the analysis of transient flows in pipe networks

G.P. Greyvenstein

School of Mechanical and Materials Engineering,Potchefstroom University for Christian Higher Education, Private Bag X6001, Potchefstroom, South Africa

SUMMARY

Existing methods for the analysis of transient flows in pipe networks are often geared towards certain types of flows such as gas flows vis-à-vis liquid flows or isothermal flows vis-à-vis non-isothermal flows. Also, simplifying assumptions are often made which introduce inaccuracies when the method is applied outside the domain for which it was originally intended. This paper describes an implicit finite difference method based on the simultaneous pressure correction approach which is valid for both liquid and gas flows, for both isothermal and non-isothermal flows and for both fast and slow transients. The problematic convective acceleration term in the momentum equation, often neglected in other methods, is retained but eliminated by casting the momentum equation in an alternative form. The accuracy and stability of the method, depending on a time-step weighing factor α, are illustrated by analizing fast transients in a pipeline and simple branching network. The proposed method compares very well with the second order Method of Characteristics and the two-step Lax-Wendroff method. The advantages of the present method is its speed over a range of problems including both fast and slow transients, its accuracy, its stability and its flexibility.

1. Introduction

Previous work on the analysis of transient flows in networks focussed mainly on specific types of flows such as liquid flows, gas flows, flows in pipelines (as opposed to flow through non-pipe components such as pumps and valves) or isothermal flows. Although these methods are suitable for the types of flow for which they were developed, they usually suffer limitations when applied to other types of flows. An example is the popular Method of Characteristics (MOC) which was initially developed to analyze fast transients in liquid pipelines (Wylie and Streeter, 1993). Although the method has been extended to deal with isothermal gas flows as well, the requirement of strict adherence to the time step-distance relationship becomes a serious limitation in the cases of non-isothermal gas flows, slow transients in gas pipelines and networks that comprise of sub-networks with different types of fluids such as heat exchanger networks. In the case of non-adiabatic gas flows the sonic velocity is not constant which implies that for fixed length increments the required time step will vary across the network. (Although it is possible to keep the time step constant and vary the length increment, it introduces additional complexities and it is not a panacea for the limitations of the MOC). In the case of slow transients many time steps are required to cover the period of interest and this slows down the simulation. In the case of heat exchangers the same length increment must be used on the hot and cold sides. If the sonic velocity of the two fluids differs, different time steps will be required for the hot and cold streams which is unacceptable.

Another example is the implicit method which is particularly suited to the analysis of gas networks where inertia forces are not as important as storage effects (Guy 1967, Amein and Chu 1975, Osiadacz 1984, Kiuchi 1994). Although the method is formulated in such a way that the relationship between time step and length increment can be relaxed, when applied to water hammer problems it is necessary to adhere to the time step-distance relationship in order to maintain a satisfactory level of accuracy. Since the implicit method requires the simultaneous solution of all the unknowns in the system at each time step, the method can become very slow when analyzing fast transients such as water hammer.

The application that prompted the development of the present method is the modeling of the power conversion unit of the Pebble Bed Modular Reactor (PBMR). This is a new type of inherently safe high temperature gas cooled nuclear reactor currently being developed by Eskom, South Africa's only utility.

The PBMR utilizes a closed circuit recuperative Brayton-cycle with helium as the working fluid to convert the heat energy to work. The recuperator and heat exchangers have to be modeled in a discretized fashion to account for heat storage effects in the metal. The pre-cooler and intercooler use water as the external fluid and it is required that the water loops be modeled as an integral part of the system. Another requirement is the ability to deal with both pipe and non-pipe components such as compressors, turbines, heat exchangers and valves. Since the intention is to use the model for both operational and accident studies it should be able to handle both slow and fast transients.

In light of these requirements if was decided to follow the implicit approach though mindful of the fact that an efficient solver for the simultaneous equations is required so as not to make it impracticably slow and not to make unnecessary simplifying assumptions that will decrease accuracy. The key features of the present method is that it can deal with both isothermal and non-isothermal flows, it can deal with both pipe and non-pipe elements and it can deal with both fast and slow transients. The method uses a time step weighing factor to balance accuracy and stability and it uses a finite volume scheme that ensures conservation of mass. Conservation of mass is an important requirement when simulating closed systems such as a Brayton-cycle power plant. Another important feature is that the problematic convective acceleration term, often omitted in other methods, is retained in the present method. The omission of this term can lead to inaccuracies in cases where there is a large variation in velocity across components such as diffusers.

A single pipeline subdivided into a number of short increments will be used to describe the method. The reason for this is that pipe elements are most commonly used and that the solution algorithm can be adequately described from the viewpoint of a simple series network.

2. Governing equations

The equations governing transient flow through a variable area duct are the continuity, the momentum and the energy equations. These equations are given in conservative form by:

Continuity:

$$\frac{\partial \rho}{\partial t} + \frac{\partial (\rho V A)}{A \partial x} = 0 \tag{1}$$

Momentum:

$$\frac{\partial (\rho V)}{\partial t} + \frac{\partial (\rho V^2 A)}{A \partial x} + \frac{\partial p}{\partial x} + \rho g \cos\theta + \frac{f \rho V |V|}{2D} = 0 \tag{2}$$

Energy:

$$\frac{\partial (\rho h_0 - p)}{\partial t} + \frac{\partial (\rho V A h_0)}{A \partial x} - \dot{q} = 0 \tag{3}$$

where h_0 is the total enthalpy defined as $h_0 = h + \frac{1}{2}V^2$.

It must be noted that Eqs. (1), (2) and (3) are only valid for rigid ducts, which is a reasonable assumption in the case of gas flows.

In order to eliminate the convective acceleration term in (2) we first use (1) to write the momentum equation in the non-conservative form. The result is:

$$\rho\frac{\partial V}{\partial t}+\rho V\frac{\partial V}{\partial x}+\frac{\partial p}{\partial x}+\rho g\cos\theta+\frac{f\rho V|V|}{2D}=0 \tag{4}$$

In the case of liquid flows we can write that

$$\begin{aligned}\rho V\frac{\partial V}{\partial x}+\frac{\partial p}{\partial x}+\rho g\cos\theta &= \frac{\partial}{\partial x}\left(p+\tfrac{1}{2}\rho V^2+\rho g z\right)\\ &= \frac{\partial p_0}{\partial x}\end{aligned} \tag{5}$$

where p_0 is the total pressure defined by $p_0 = p + \tfrac{1}{2}\rho V^2 + \rho g z$.

Substitution of (5) into (2) leads to

$$\rho\frac{\partial V}{\partial t}+\frac{\partial p_0}{\partial x}+\frac{f\rho V|V|}{2D}=0 \tag{6}$$

Using principles in gas dynamics it can be proved that for gas flows

$$\rho V\frac{\partial V}{\partial x}+\frac{\partial p}{\partial x}=\frac{p}{p_0}\frac{\partial p_0}{\partial x}+\frac{\rho V^2}{2T_0}\frac{\partial T_0}{\partial x} \tag{7}$$

where the total temperature and total pressure for gas flows are defined as:

$$T_0 = T\left(1+\frac{\gamma-1}{2}M^2\right) \qquad \text{and} \tag{8}$$

$$p_0 = p\left(1+\frac{\gamma-1}{2}M^2\right)^{\frac{\gamma}{\gamma-1}} \tag{9}$$

Substitution of (7) into (4) leads to:

$$\rho\frac{\partial V}{\partial t}+\frac{p}{p_0}\frac{\partial p_0}{\partial x}+\rho g\cos\theta+\frac{\tilde{f}\rho V|V|}{2D}=0 \tag{10}$$

where the effective friction factor $\tilde{f}$ is given by:

$$\tilde{f} = f+\frac{D}{T_0}\frac{\partial T_0}{\partial x}\frac{V}{|V|} \tag{11}$$

The second term on the right of (11) is usually much smaller than f and in the case of adiabatic flow it will be exactly zero. However, in the case of combusting flows the term may become significant and will therefore be retained.

The equations governing gas flow are (1), (6) and (3) while the equations governing liquid flow are (1), (10) and (3).

In the case of gas flow we also need an equation of state that expresses the pressure in terms of density and temperature. Such an equation of state is:

$$p = s\rho RT \tag{12}$$

where R is the gas constant and *s* is the compressibility factor.

Although the method presented in this paper is valid for both liquid and gas flows, for the sake of brevity, we will only describe the gas flow variant of the method.

3. Discretization of governing equation

Finite volume discretization, as shown in Figure 1, is used to transform the partial differential equations into a set of algebraic equations. Pressures, densities and temperatures are defined at cell centers while velocities and volumetric flow rates are defined at cell boundaries.

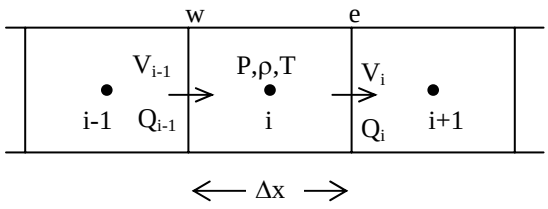

Figure 1: Finite volume discretization scheme

Integration of the continuity equation over control volume *i* leads to:

$$\forall_i \frac{(\rho_i - \rho_i^o)}{\Delta t} + \alpha\left(\rho_e Q_i - \rho_w Q_{i-1}\right) + (1-\alpha)\left(\rho_e Q_i - \rho_w Q_{i-1}\right)^o = 0 \tag{13}$$

where Q is the volumetric flow rate and $\forall$ is the volume of the control volume. Subscripts *e* and *w* refer to values to the right and left at the control volume boundaries as shown in Figure 2. Superscript *o* refers to the previous time level, t, while values or terms without any superscript are taken at the new time level (t +Δt). α is a weighing factor between the previous and the present time levels and its value can vary between 0 and 1. With α=0 the scheme becomes fully explicit and with α=1 the scheme becomes fully implicit. If α=0.5 the time integration is equivalent to that of the second order Crank-Nicholson method (Roach 1972). The present method, however, becomes unstable when α < 0.5 so that in practice α can only be varied between 0.5 and 1. For α=1 the method is first order accurate in time while for α=0.5 it is second order accurate. For α-values close to 0.5 the scheme sometimes becomes unstable and an α-value of 0.6 offers a good compromise between accuracy and stability.

Integration of (10) over a control volume centered at interface *e* leads to:

$$\begin{aligned}\frac{\rho_e \Delta x}{A_e}\frac{(Q_i - Q_i^o)}{\Delta t} + \alpha\left(\frac{p_e}{p_{0_e}}(p_{0_{i+1}} - p_{0_i}) + \rho_e g\Delta x\cos\theta + \frac{\tilde{f}\,\Delta x\rho_e Q_i|Q_i|}{2DA_e^2}\right) + \\ (1-\alpha)\left(\frac{p_e}{p_{0_e}}(p_{0_{i+1}} - p_{0_i}) + \rho_e g\Delta x\cos\theta + \frac{\tilde{f}\,\Delta x\rho_e Q_i|Q_i|}{2DA_e^2}\right)^o = 0\end{aligned} \tag{14}$$

where A_e is the cross sectional area at cell face *e*.

Integration of (3) over control volume *i* leads to:

$$\forall_i\left(\frac{\rho_i h_{0_i}-\rho_i^o h_{0_i}^o}{\Delta t}\right)-\forall_i\left(\frac{p_i-p_i^o}{\Delta t}\right)+\alpha(\rho_e Q_i h_{0_e}-\rho_w Q_{i-1}h_{0_w})+(1-\alpha)(\rho_e Q_i h_{0_e}-\rho_w Q_{i-1}h_{0_w})^o=\forall_i \dot{q} \tag{15}$$

Equation (12) to (15) need to be solved simultaneously for all the unknowns p_{0_i}, Q_i, h_{0_i} and ρ_i at the new time level given their values at the previous time level and at the boundaries.

4. Solution algorithm

The solution algorithm is an extension of the steady-state pressure correction method described by Greyvenstein and Laurie (1994). Following this approach we first use a field of guessed or preliminary pressures $\overline{p}_{0_i}$ to solve for preliminary flow rates $\overline{Q}_i$ using (14) and preliminary densities $\overline{\rho}_i$ using (12). For the first iteration one can use the pressure field from the previous time level and for later iterations one can use the pressures from the previous iteration.

Next one needs to determine a field of corrected pressures, flow rates and densities that better satisfy (12), (13) and (14). Towards this end we write that:

$$\begin{aligned} p_0 &= \overline{p}_0 + p_0' \\ Q &= \overline{Q} + Q' \\ \rho &= \overline{\rho} + \rho' \end{aligned} \tag{16}$$

where overbars denote preliminary values and accents denote corrections.

The density correction can be related to the pressure correction using the equation of state:

$$\rho' = \frac{p_0'}{sRT}\frac{p}{p_0} \tag{17}$$

Subtracting (14) with the preliminary values substituted into it, from (14) with the corrected values (16) substituted into it, and neglecting terms involving products of corrections we get:

$$\frac{\overline{\rho}_e \Delta x}{A_e}\frac{Q_i'}{\Delta t}+\frac{\rho_e' \Delta x}{A_e}\frac{\overline{Q}_i}{\Delta t}+\alpha\left(\frac{p_e}{p_{0_e}}(p_{0_{i+1}}'-p_{0_i}')+\rho_e' g \Delta x\cos\theta+\frac{\tilde{f}\,\Delta x \rho_e' \overline{Q}_i\left|\overline{Q}_i\right|}{2DA_e^2}+\frac{\tilde{f}\,\Delta x \overline{\rho}_e 2Q_i'\left|\overline{Q}_i\right|}{2DA_e^2}\right)=0 \tag{18}$$

Using (12) we can write that:

$$\rho_e' = 0.5(p_{0_i}' + p_{0_{i+1}}')sRT_e\, p_e / p_{0_e} \tag{19}$$

Substituting (19) into (18) and solving for Q_i':

$$Q_i' = a_e^- p_{0_i}' - a_e^+ p_{0_{i+1}}' \tag{20}$$

where

$$a_e^+ = \frac{p_e}{p_{0_e}}\left[\alpha + \frac{sRT_e\Delta x}{2}\left(\frac{\overline{Q}_i}{A_e\Delta t} + \alpha g\cos\theta + \frac{\alpha\tilde{f}\overline{Q}_i\left|\overline{Q}_i\right|}{2DA_e^2}\right)\right] \Bigg/ \left[\frac{\rho_e\Delta x}{A_e\Delta t} + \frac{\alpha\tilde{f}\Delta x\overline{\rho}_e\left|\overline{Q}_i\right|}{2DA_e^2}\right] \tag{21}$$

$$a_e^- = \frac{p_e}{p_{0_e}}\left[\alpha - \frac{sRT_e\Delta x}{2}\left(\frac{\overline{Q}_i}{A_e\Delta t} + \alpha g\cos\theta + \frac{\alpha\tilde{f}\overline{Q}_i\left|\overline{Q}_i\right|}{2DA_e^2}\right)\right] \Bigg/ \left[\frac{\rho_e\Delta x}{A_e\Delta t} + \frac{\alpha\tilde{f}\Delta x\overline{\rho}_e\left|\overline{Q}_i\right|}{2DA_e^2}\right] \tag{22}$$

Substitution of (16) into the continuity equation (13) leads to:

$$\begin{aligned} &\forall_{\mathrm{i}}\frac{\rho_i'}{\Delta t} + \alpha(\rho_e'\overline{Q}_i + \overline{\rho}_e Q_i' - \rho_w'\overline{Q}_{i-1} - \overline{\rho}_w Q_{i-1}') + \\ &\forall_{\mathrm{i}}\frac{(\overline{\rho}_i - \rho_{i-1}^o)}{\Delta \mathrm{t}} + \alpha\left(\overline{\rho}_e\overline{Q}_i - \overline{\rho}_w\overline{Q}_{i-1}\right) + (1-\alpha)\left(\rho_e Q_i - \rho_w Q_{i-1}\right)^o = 0 \end{aligned} \tag{23}$$

We now substitute (19) and (20) along with similar equations for ρ_w' and Q_{i-1}' into (23) to get the following equation for pressure correction:

$$c_P\, p_{0_i}' = c_E\, p_{0_{i+1}}' + c_W\, p_{0_{i-1}}' + b_i \tag{24}$$

where

$$c_E = \alpha\left(\overline{\rho}_e a_e^+ - \frac{\overline{Q}_i}{2sRT_e}\right) \tag{25}$$

$$c_W = \alpha\left(\overline{\rho}_w a_w^- + \frac{\overline{Q}_{i-1}}{2sRT_w}\right) \tag{26}$$

$$c_P = \left[\frac{\forall_{\mathrm{i}}}{sRT_i}\frac{p_i}{p_{0_i}} + \alpha\left(\overline{\rho}_e a_e^- + \overline{\rho}_w a_w^+ + \frac{\overline{Q}_i}{2sRT_e} - \frac{\overline{Q}_{i-1}}{2sRT_w}\right)\right] \tag{27}$$

$$b_i = -\left[\forall_{\mathrm{i}}\frac{(\overline{\rho}_i - \rho_{i-1}^o)}{\Delta \mathrm{t}} + \alpha\left(\overline{\rho}_e\overline{Q}_i - \overline{\rho}_w\overline{Q}_{i-1}\right) + (1-\alpha)\left(\rho_e Q_i - \rho_w Q_{i-1}\right)^o\right] \tag{28}$$

In the case of a single pipeline (24) can be solved with the Thomas algorithm (Anderson, Tannehill and Pletcher, 1984) while sparse matrix techniques can be employed in the case of complex pipe networks.

With the field of p_0'-values known, new updated values for p_0, Q and ρ are determined using (16), (17) and (20). The newly updated values are now treated as the preliminary values for the next iteration and the whole process repeated a number of times after which the energy equation is solved.

Following the upstream approach for the terms h_{0_e} and h_{0_w} in (15) and using (13), the energy equation can be written in the following form:

$$k_P\, h_{0_i} = k_E\, h_{0_{i+1}} + k_W\, h_{0_{i-1}} + k_t\, h_{0_i}^o + r_i \tag{29}$$

where

$$k_E = -\alpha \rho_e Q_i \quad \text{if} \quad Q_i < 0$$
$$= 0 \quad \text{if} \quad Q \geq 0 \tag{30}$$

$$k_W = \alpha \rho_w Q_{i-1} \quad \text{if} \quad Q_{i-1} \geq 0$$
$$= 0 \quad \text{if} \quad Q_{i-1} < 0 \tag{31}$$

$$k_t = \frac{\forall_i \rho_i^o}{\Delta t} \tag{32}$$

$$k_P = k_E + k_W + k_t + (1-\alpha)(\rho_e Q_i - \rho_w Q_{i-1})^o \tag{33}$$

$$r_i = \forall \left(\dot{q} + \frac{p_i - p_i^o}{\Delta t} \right) - (1-\alpha)(\rho_e Q_i h_{0_e} - \rho_w Q_{i-1} h_{0_w})^o \tag{34}$$

In the case of a single pipeline Eq. (26) can be solved with the Thomas algorithm while sparse matrix techniques can be used in the case of complex networks.

The alternate solutions of (24) and (29) are repeated until convergence. The whole process is repeated for the next and subsequent time steps until the simulation period has been covered.

5. Numerical examples

5.1 Steady state examples

Although the method will primarily be used for transient simulations, its ability to accurately predict steady-state flows is very important since the steady-state solution is often used as the initial condition for transient simulations.

In the case of steady-state flow the equations of motion of an ideal gas through a constant area pipe can be reduced to the following set of ordinary differential equations (Saad, 1985):

$$\frac{dM^2}{M^2} = (1+\gamma M^2) B \frac{dT_0}{T_0} + \gamma M^2 A f \frac{dx}{D} \tag{35}$$

$$\frac{dT}{T} = (1-\gamma M^2) B \frac{dT_0}{T_0} - \frac{\gamma(\gamma-1)M^4}{2(1-M^2)} f \frac{dx}{D} \quad \text{and} \tag{36}$$

$$\frac{dp_0}{p_0} = -\left(\frac{dT_0}{T_0} + f \frac{dx}{D} \right) \gamma M^2 \tag{37}$$

where

$$B = \frac{\left(1 + \frac{\gamma-1}{2} M^2\right)}{1-M^2}$$

Numerical integration of (35) to (37) over a pipeline subdivided into a number of increments yields a benchmark steady-state solution.

The situation that will be considered is helium flowing through a 100 m long, 0.5 m diameter pipeline with an inlet temperature of 300K and an outlet total pressure of 200 kPa. The friction factor is assumed to be constant with $f = 0.02$ while 20 length increments are used in all cases. Initially all pressures, except the inlet pressure, are set equal to the outlet pressure while the initial velocities are zero.

Figure 2 compares the pressure ratio as function of outlet Mach number of four methods to that of the benchmark solution (Num) for the case of isothermal flow. The first method is the present method (PC), the second is the two-step Lax-Wendroff method (LW), the third is the MOC where the convective acceleration term has been retained (MOC1) and the fourth is the MOC where the convective acceleration term has been neglected (MOC2). The PC, LW and MOC1 methods agrees very well with the benchmark solution while MOC2 starts to deviate from the benchmark solution at outlet Mach numbers larger than 0.3. At an outlet Mach number of 0.7 the pressure ratio error is approximately 13 percent. This demonstrates the significance of the convective acceleration term at higher Mach numbers.

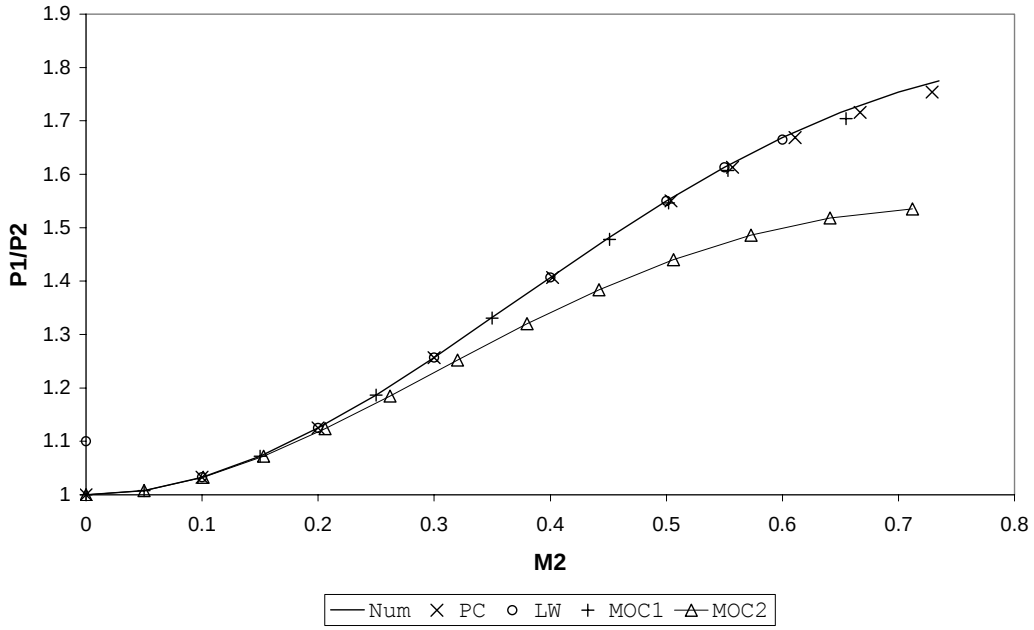

Figure 2: Pressure ratio as function of outlet Mach number of various methods for the case of isothermal steady-state flow through a 100 m long pipeline.

Figure 3 compares the pressure ratio as function of outlet Mach number and overall temperature difference of the present method to that of the benchmark solution for the case of non-isothermal flow. The present method agrees very well with the benchmark solution.

The execution time for a typical steady-state simulation on a 366 MHz Pentium II processor is less than 0.1 seconds for all three methods. This makes it difficult to draw definitive conclusions on the relative speed of the three methods. More will, however, be said on the relative speed of the three methods in the next sections that deal with transient examples.

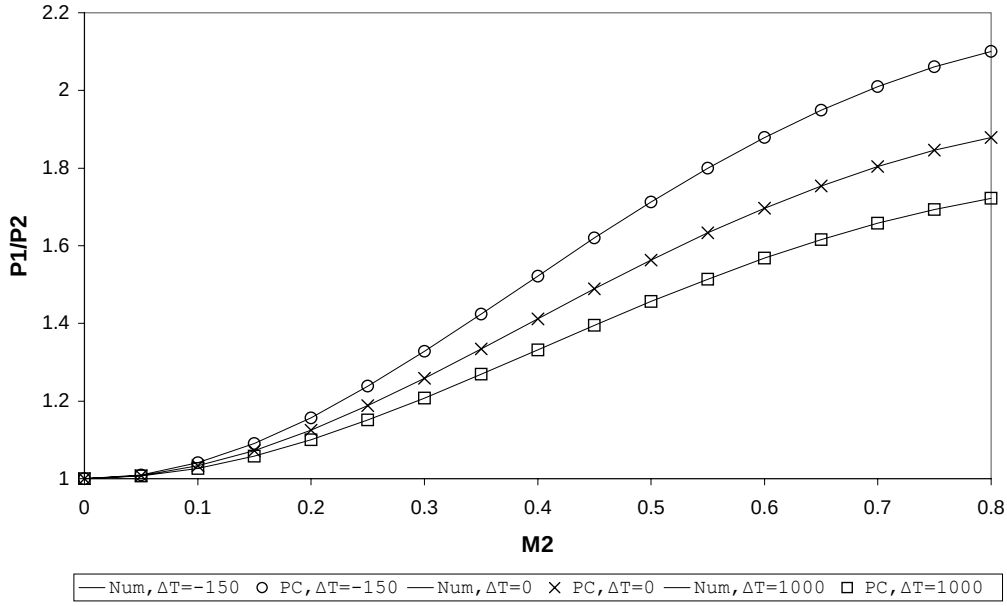

Figure 3: Pressure ratio as function of outlet Mach number and overall temperature difference for the case of non-isothermal steady-state flow through a 100 m long pipeline.

5.2 Sudden closure of a valve in a single pipeline

In this example the pressure pulses due to the sudden closure of a valve at the downstream end of a 20 m, 0.5 m diameter pipe is simulated. The fluid is helium. The simulation starts with the steady-state solution in which the inlet pressure is 700 kPa, the inlet temperature is 300 K and the mass flow rate is 44.86 kg/s. This gives an outlet Mach number of 0.21 prior to the closing of the valve. A constant friction factor of 0.02 is used while the pipe is divided into 20 increments.

Figure 4 shows the pressure variation at the downstream end of the pipe for the case of isothermal flow. The results of the following methods are presented: the present method with a time integration factor α of 1, the present method with α=0.6, the MOC and the two-step Lax-Wendroff method. In the case of the MOC the convective acceleration term is neglected. The reason for this is that the method becomes unstable if this term is retained. A time step of 0.0009 seconds was used for both the present method and the LW method, which is approximately 70 percent of the MOC time step.

Referring to Figure 4, the MOC shows a very abrupt change between the peak and trough values with a resultant block-like wave shape while in the case of the other methods the pressure waves have a more sinusoidal shape. This block-like wave shape of the MOC is partly due to the omission of the convective acceleration term. Considering only the amplitude and frequency of the pressure waves (and not the shape of the waves) it can be concluded that the MOC, the two-step Lax-Wendroff method and present method with α=0.6 compare very well. The present method with α=1 exhibits a larger dampening of the pressure wave. This is due to the numerical approximation error of the time derivative term. This error cannot be reduced by refining the grid spacing as α has no effect on the accuracy of the spacial derivative term. An obvious method to reduce the numerical approximation error is to decrease the time step. This will, however, slow down execution time. A better approach is therefore to decrease the value of α.

With α=1 the present method is only first order accurate in time while it is second order accurate when α=0.5. The method, however, becomes unstable for α-values close to 0.5 and it was found that an α-value of 0.6 offers a good compromise between accuracy and stability.

The execution times of the different methods for a 2 second simulation period were as follows: MOC, 0.4 s; two-step Lax-Wendroff method, 0.7 s; and the present method, 20 s. This implies that the present method is approximately 30 times slower than the two-step Lax-Wendroff method and 50 times slower than the MOC. It should, however, be kept in mind that the present example represents a fast transient case where the time step of the present method had to be made approximately the same as that of the two explicit method to achieve the same level accuracy as these methods. However, in the case of slow transients the time step of the implicit method can be made much larger than that of the explicit methods without significant loss of accuracy, which makes the implicit method faster than the explicit methods in the case of slow transients. This will be illustrated in the Section 5.4. Although the present method will mainly be used for the analysis of slow transients it is important to know that its accuracy is comparable to that of second order explicit methods in the case of fast transients.

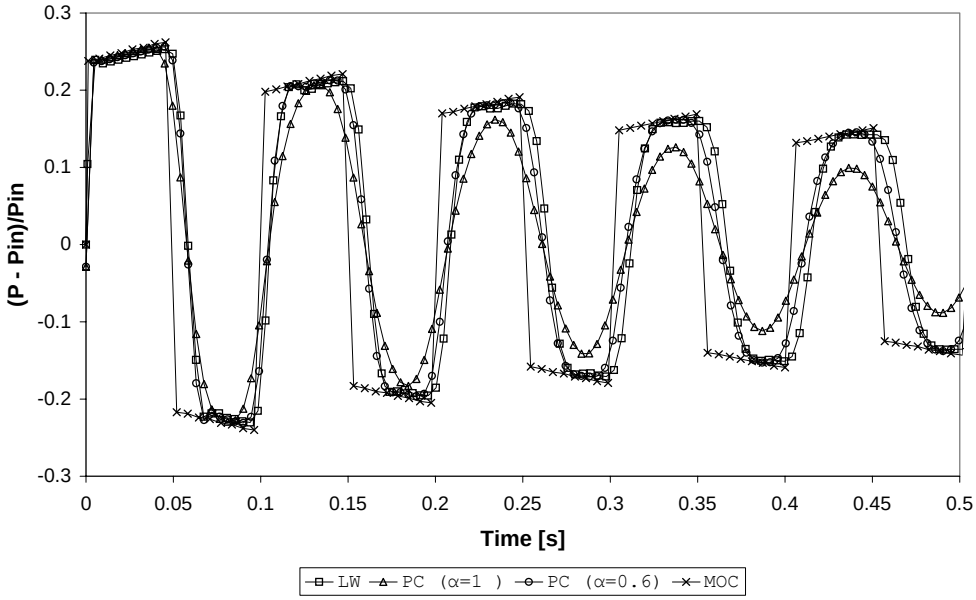

Figure 4: Variation of pressure at the end of a 20 m long, 0.5 m diameter pipe due to the sudden closure of a valve at the downstream end of the pipe for the case of isothermal flow.

Figure 5 shows the effect of number of length increments, n, on the pressures at the downstream end of the pipe. In the case of both the MOC and the present method the solutions for n=10 (Δx =2m) and n=20 (Δx =1m) are virtually identical while for the two-step Lax-Wendroff method the solutions for n=10 and n=20 are noticeably different. The reason for this difference is due to numerical round-off errors associated with the finite difference approximation of the convective acceleration term. (The convective acceleration term consists of a spatial derivative). This error increases as the length increment increases. The reason why the solutions for n=10 and n=20 are the same in the case of the MOC is that the convective acceleration term, which is the source of the round-off errors, is omitted in the case of the MOC. In the case of the present method the convective acceleration term is eliminated by working with the total pressure instead of the static pressures as discussed in Section 2. This explains why the solutions for n=10 and n=20 are also the same in the case of the present method.

Figure 6 and 7 compare the pressure and temperature variation of the present method with that of the two-step Lax-Wendroff method for the case of adiabatic flow. Again the present method with α=1 exhibits larger numerical dampening while the present method with $\forall$=0.6 agrees very well with the two-step Lax-Wendroff method.

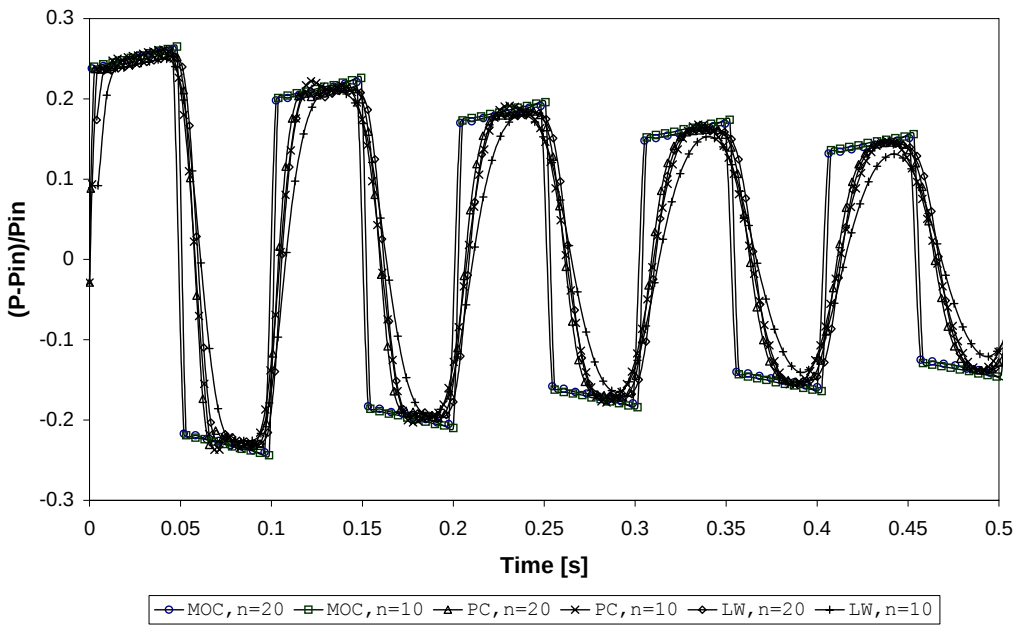

Figure 5: Effect on number of increments, n, on the pressure variation at the downstream end of the pipe.

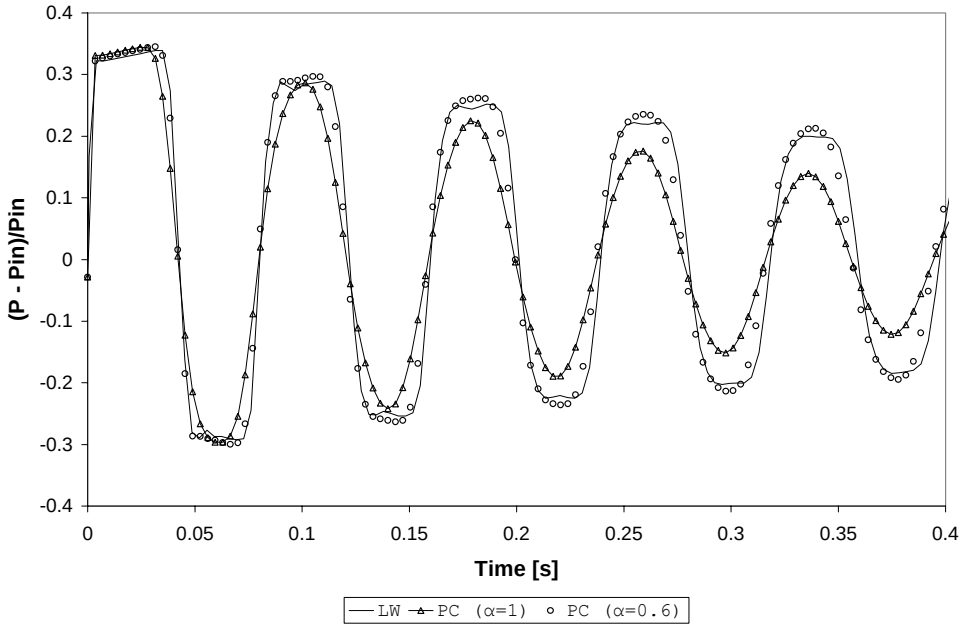

Figure 6: Variation of pressure at the end of a 20 m long, 0.5 m diameter pipe due to the sudden closure of a valve at the downstream end of the pipe for the case of adiabatic flow.

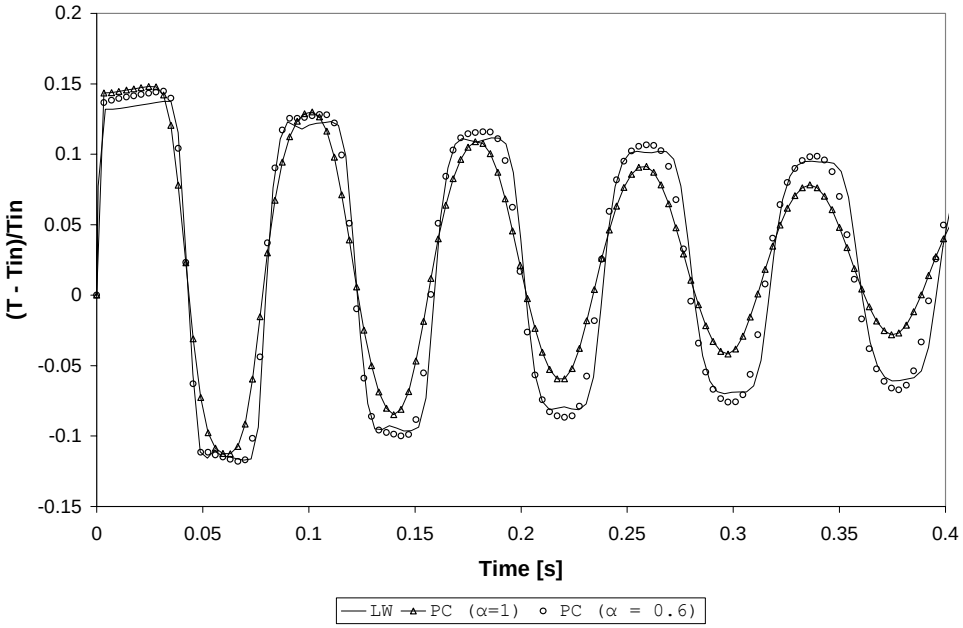

Figure 7: Variation of temperature at the end of a 20 m long, 0.5 m diameter pipe due to the sudden closure of a valve at the downstream end of the pipe for the case of adiabatic flow.

5.3 Sudden closure of valves in a simple branching network

This example involves a simple branching network as shown in Figure 8. The network consists of 5 pipes, each 10 m long and 0.5 m in diameter. A constant length increment of 1 m is used implying 10 increments per pipe or 50 increments in total. The fluid in helium. The simulation starts with the steady-state solution in which the inlet pressure is 700 kPa, the temperature is 300 K, the mass flow rate in branch 1 is 11.61 kg/s and the mass flow rates in branches 2 and 3 are 12.37 kg/s. At time zero, valves at the end of branches 1 and 2 are suddenly close while the mass flow out of branch 3 is kept constant at the steady-state value. The total pressure at the inlet is also kept constant at the steady-state value while the flow is assumed to be isothermal.

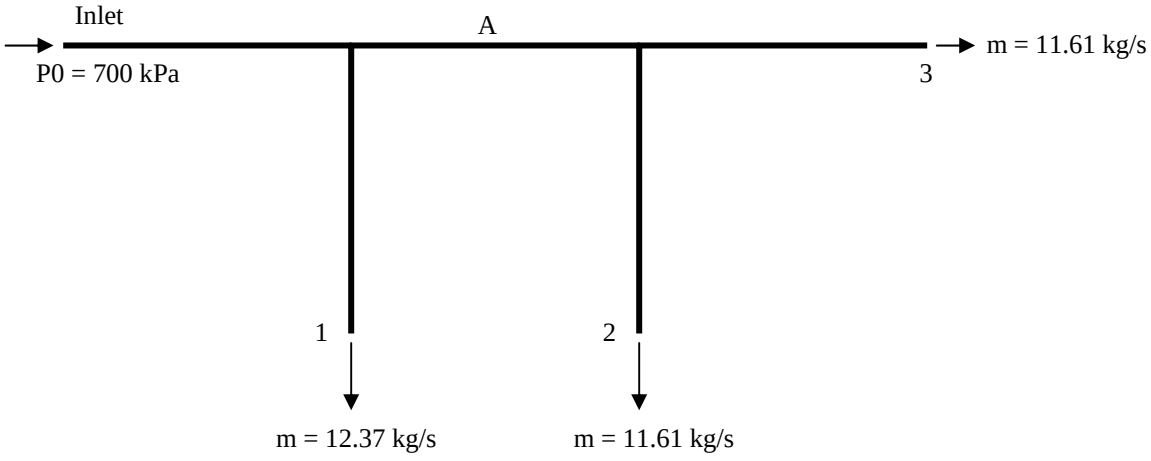

Figure 8: Network example.

Figure 9 shows the pressure variation at position A (which is halfway between the two branch-off points) in the network for the present method, the MOC and the two-step Lax-Wendroff method. In the case of the present method and the two-step Lax-Wendroff method a time increment of 0.0009 was used while a time integration weighing factor of α=0.6 was used for the present method.

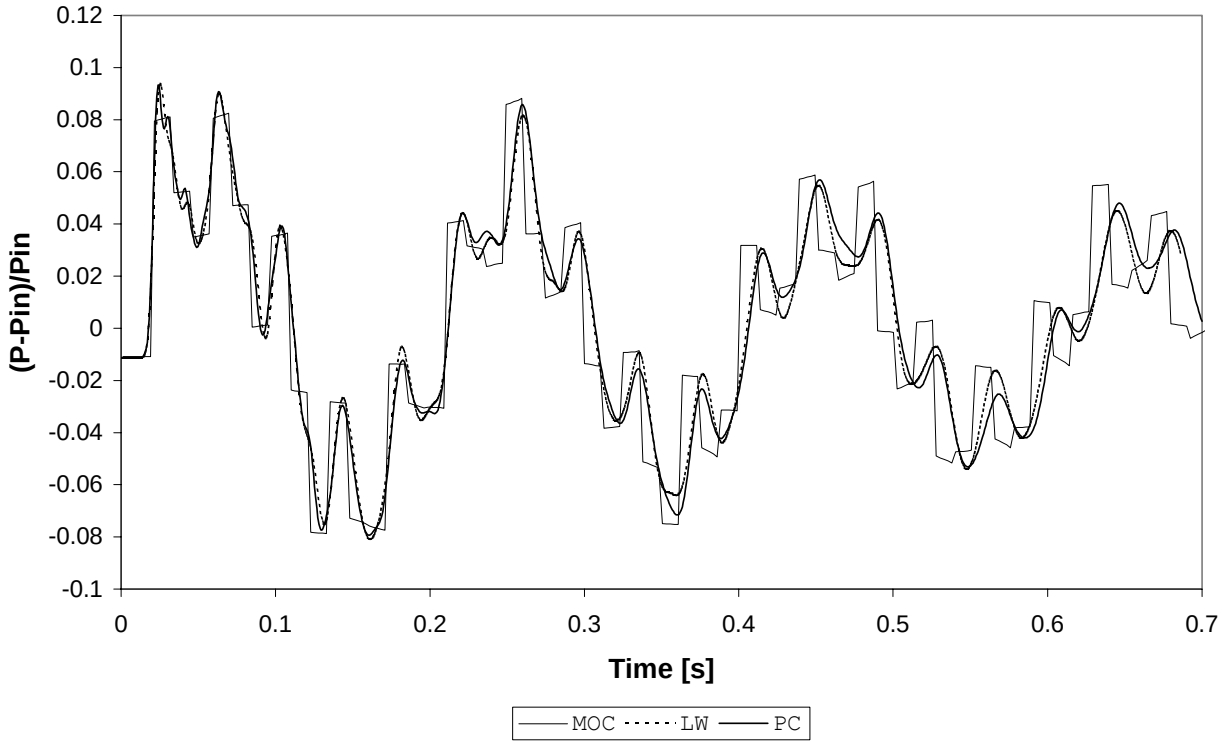

Figure 9: Pressure variation at position A in the network shown in Figure 8.

The present method agrees well with the two-step Lax-Wendroff method, especially for times up to about 0.33 seconds. Thereafter the differences in the peak and trough values become more pronounced. However, the results do not diverge and later on some of the peak and trough values are very close. What is especially encouraging, from a design point of view, is the close agreement in the peak and trough values during the first couple of cycles.

The agreement is quite good if one keeps in mind that in a network discrepancies are not only due to differences in the basic methodologies but also due to differences in how the junctions are treated. Although the treatment of junctions is very straight forward in the case of the present method it is not so straight forward in the case of the two-step Lax-Wendroff method.

The present method also compares well with the MOC although a slight time shift starts to appear after about 0.3 seconds.

5.4 Blow-down of a pressure vessel through a pipe

The last example that will be considered is that of a pressure vessel blowing down into a second pressure vessel through a 10 m long, 0.1 m diameter pipe with a constant friction factor of f = 0.02. The fluid is helium at a constant temperature of 300 K. The pressure in the upstream pressure vessel varies according to

$$p_1 = 650 + 50e^{-0.004t} \text{ kPa}$$

while the pressure in the downstream vessel is kept constant at p_2=650 kPa.

The pipe was subdivided into 40 constant increments of 0.25 m each while the simulation was carried out over a period of 30 minutes. The reason why a pipe increment of 0.25 m was chosen is because this typifies the shortest pipe run in the plant under consideration (the PBMR). The shortest pipe run determines the maximum time step in the case of the explicit methods.

The reason why the simulation was carried out over a period of 30 minutes is because this is a typical period over which simulations have to be carried out for the PBMR.

The MOC time step for this problem was $\Delta x / \sqrt{RT} = 0.003165$ while a time step of 0.0025 s was used for the two-step Lax-Wendroff method. This is the largest time step that still gives a stable solution. In the case of the present method the time step is not limited by the time step-distance relationship and a rather large value of 10 s was used. This value was determined as a trade-off between speed and accuracy.

Figure 10 shows the variation of mass flow over time for the MOC, the two-step Lax-Wendroff method, and the present method. All three methods compare very well. The slight difference between the MOC and the other two methods is due to the omission of the convective acceleration term in the case of the MOC.

The execution times for the three methods were as follows: MOC, 180s; two-step Lax-Wendroff method, 2945 s; and the present method, 2.5 s. This implies that the present method is 72 times faster than the MOC and 1178 times faster than the two-step Lax-Wendroff method for this example. This illustrates the advantage of the present implicit method over explicit methods in the case of slow transients.

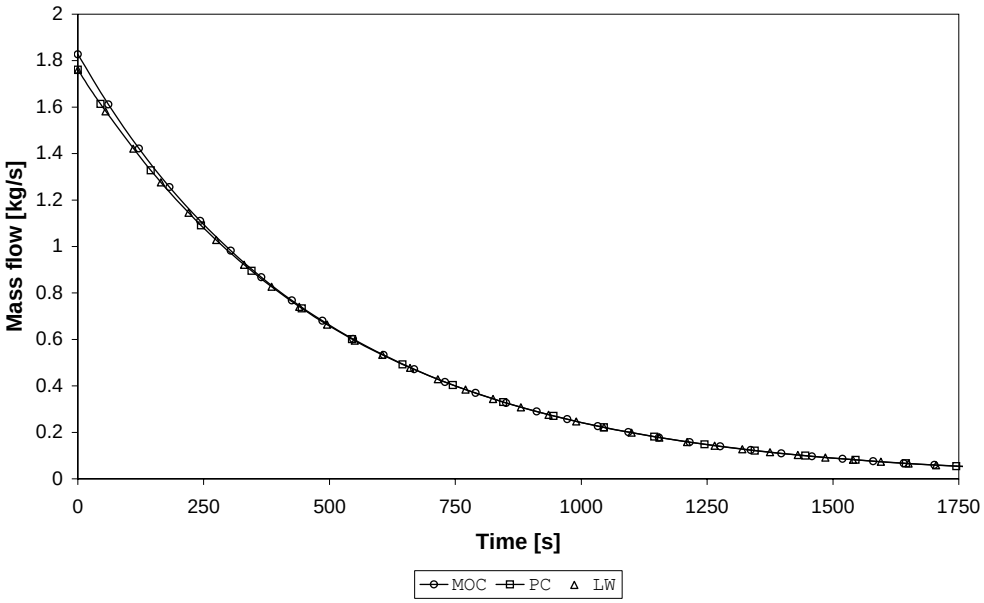

Figure 10: Comparison of mass flow as function of time for the MOC, the two-step Lax-Wendroff method (LW) and the present method (PC).

6. Conclusion

An implicit finite difference method for the prediction of transient flows in pipe networks has been presented in this paper. The method retains the problematic convective acceleration term in the momentum equation, often neglected in other methods. This term has a significant impact on accuracy in the case of high speed flows. Although the method is suitable for both liquid and gas flows, for both isothermal and non-isothermal flows and for both fast and slow transients, only its application to gas flows has been demonstrated in this paper. The method incorporates a time step weighing factor α which can be varied between 0.5 and 1. For α=1 the method is first order accurate in time while it becomes second order accurate when α=0.5. Increased accuracy, however, comes at the expense of stability and an α-value of 0.6 offers a good compromise between accuracy and stability. With an α-value of 0.6 the present method compares very well with the second order two-step Lax-Wendroff method. Although the method is slower than explicit methods when applied to fast transients, it is faster than explicit methods in the case of slow transients.

The main advantages of the present method are its average speed over a range of problems including both fast and slow transients, its accuracy and its stability. The method is also very flexible and it has been extended to deal with a large variety of non-pipe components such as compressors, turbines, orifices, pumps and heat exchangers. The extended method forms the basis of a simulation model for the power conversion unit of the Pebble Bed Modular Reactor (PBMR), a new type of high temperature gas cooled reactor currently being developed in South Africa.

7. Acknowledgements

Part of this work has been carried out while the author visited the Department of Mechanical and Materials Engineering of the University of Western Australia. The author gratefully acknowledges the support of the University of Western Australia for this work.

Notation

A = cross sectional area of duct
c_v = constant volume specific heat
c_p = constant pressure specific heat
D = pipe diameter
f = Darcy friction factor
$\tilde{f}$ = effective friction factor
g = gravitational acceleration
h = enthalpy
M = Mach number
n = number of length increments
p = pressure
$\dot{q}$ = heat transfer per unit volume
Q = volumetric flow rate
R = ideal gas constant
s = compressibility factor
t = time
T = temperature
V = velocity
$\forall$ = volume
x = distance along pipe
α = time step weighing factor
Δ = increment
ρ = density
θ = angle between centerline of pipe and the vertical

γ = ratio of specific heats of gas i.a. c_p/c_v

Subscripts

0 = total values
e = control volume boundary values on the right hand side of the control volume
w = control volume boundary values on the left hand side of the control volume

Superscripts

o = previous time level
' = correction

Abbreviations

LW = two-step Lax-Wendroff method
MOC = Method of Characteristics
Num = Numerical solution
PBMR = Pebble Bed Modular Reactor (a new type of inherently safe high temperature gas cooled nuclear reactor currently being developed in South Africa)
PC = pressure correction method (present method)

References

Amein, M. and Chu, H. L. 1975. Implicit numerical modeling of unsteady flows. J. Hydraul. Div., ASCE, **102**, No. HY1, 29-39

Anderson, D. A., Tannehill, J. C. and Pletcher, R. H. 1984. *Computational Fluid Mechanics and Heat Transfer*. Hemisphere Publishing Corporation, New York

Greyvenstein, G. P. and Laurie, D. P. 1994. A segregated CFD approach to pipe network analysis. *Int. J. Numer. Methods E.*, **37**, 3685 - 3705

Guy, J. J. 1967. Computation of unsteady gas flow in pipe networks. *I. Chem. E.*, Symp. Series 23, 139-145

Kiuchi, T. 1994. An implicit method for transient gas flows in pipe networks. *Int. J. Heat and Fluid Flow.*Vol. 15, No. 5, October, 378-383

Osiadacz, A. 1984. Simulation of transient gas flows in networks. *Int. J. Numer. Methods Fluid*, **4**, 13-23

Roach, P. 1972. *Computational Fluid Dynamics.*Hermosa Publishers. Albuquerque, NM

Saad, M.A. 1985. *Compressible Fluid Flow.* Prentice Hall, New York

Wylie, E. B. and Streeter, V. L. 1993. *Fluid Transients in Systems.* Prentice Hall, Englewood Cliffs, NJ

C:\DOCS\Artikels\Implic3.doc